NOx REDUCTION IN DIESEL FUEL FLAMES BY ADDITIONS OF WATER AND CO_2

S.C. Li
University of California - San Diego

INTRODUCTION

Natural gas, composed mostly of methane, CH_4, has been called the 'prince' of hydrocarbon fuels [1]. Global natural gas reserves have kept on increasing rapidly. For example, global reserves of natural gas increased from 40 billion tons in 1970 to 130 billion tons in 1992 while global oil reserves increased from 70 billion tons to 140 billion tons in the same time period. This means that natural gas will remain cheap and abundant in the future. Natural gas has the highest heating value per unit mass (50.1 MJ/kg, LHV) of any of the hydrocarbon fuels (e.g., butane, liquid diesel fuel, gasoline, etc). Since it has the lowest carbon content per unit mass, combustion of natural gas produces much less carbon dioxide, soot particles, and oxide of nitrogen than combustion of liquid diesel fuel. In view of anticipated strengthening of regulations on pollutant emissions from diesel engines, alternative fuels, such as compressed natural gas (CNG) and liquefied natural gas (LNG) have been experimentally introduced to replace the traditional diesel fuels in heavy-duty trucks, transit buses, off-road vehicles, locomotives, and stationary engines [2]. In the 1997 SAE Future Transportation Technology Conference, there were more than 12 papers which addressed the possibility of natural gas as a major fuel for future diesel engines. To help in applying natural gas in Diesel engines and increasing combustion efficiency, the emphasis of the present paper is placed on the detailed flame chemistry of methane-air combustion. The present work is our continued effort [3] in finding better methods to reduce No_x. The goal is to identify a reliable chemical reaction mechanism for natural gas in both premixed and diffusion flames and to establish a systematic reduced mechanism which may be useful for large-scale numerical modeling of combustion behavior in natural gas engines.

NUMERICAL COMPUTATION AND MODELING

1. Numerical Integrations

We confine our attention to the neighborhood of the axis in an axisymmetric counterflowing configuration, as shown in Figure 1, where the axial velocity, and state variables depend on the axial coordinate only and the radial velocity is linear in radial coordinate and the pressure p depends on both coordinates in a special manner so that all the governing equations can be reduced to ordinary differential equations as discussed by Smooke et al. [4]. The numerical integrations apply to laminar flames with potential flow in the outer streams. Only the radiation from CO, CO_2 and H_2O is taken into account in the energy equation.

The integrations with detailed chemistry and transport included are performed employing a numerical code developed at RWTH, Aachen, Germany [5]. This code was modified locally to include the effects of droplet vaporization in the energy equation. In the present paper, we report results for a strain rate of $50s^{-1}$ at atmospheric pressure. The equivalence ratio is varied from $\Phi = 1.5$ to $\Phi = 3.0$. For diffusion flame, $\Phi = \infty$.

2. Chemical Reaction Mechanism

The reaction mechanism used in the numerical computations starts with $H_2/0_2$ combustion and is constructed by subsequently incorporating wet-CO oxidation and CH_4 flame chemistry, including formation and oxidation of C_2 and C_3 species. Reaction mechanisms in $H_2/0_2$ and $H_2/0_2/CO$ combustion systems have been thor-oughly evaluated earlier [6, 7, 8] and the resulting compilation is adopted here without modification. Oxidation mechanisms for methane and No_x chemistry are compiled and validated by the experiments of freely propagating flames and by our recent work on two-stage partially premixed

methane flames [9]. This detailed reaction mechanism consists of 224 elementary reactions among 50 species which are:

CH_4, O_2, CO, CO_2, H_2, H_2O, H, OH, O, HO_2, H_2O_2, CH, CHO, CHCO, $^1CH_2$, $^3CH_2$, CH_2O, CH_3, CH_3OH, CH_3O, CH_2OH, C_2H, C_2H_2, C_2H_3, C_2H_4, C_2H_5, C_2H_6, HCCO, CH_3CO, C_3H_3, C_3H_4, C_3H_5, C_3H_6, i-C_3H_7, n-C_3H_7, C_3H_8, N, NH, NH_2, NH_3, NO, HNO, HCN, HNCO, NCO, CN, NO_2, N_2, N_2H, N_2O.

EXPERIMENT

1. Two-Phase Counterflow Burner

The burner, which has two coaxial ducts placed one above the other, is shown in Figure 1. The single-phase methane-air gas mixture flows through the upper duct and the water spray with air through the lower duct. The separation distance between the upper and lower duct exits is 18 mm. The upper duct has an exit diameter of 45 mm and flow straighteners are installed to produce a uniform gas flow at the exit plane. The lower duct is a long contoured tube with the same exit diameter. An atomizer is located at the bottom of the lower duct to produce water spray. The air enters the duct below the spray nozzle and carries the spray upward to meet the gas flow from the upper duct. Since some droplets are lost to the walls or to the bottom of the lower duct, a liquid-fuel drain pipe is installed to discharge the accumulated liquid. The mass flow rate of water in the counterflow is obtained as a function of the flow rate of the carrier gas by metering the water flowing into the atomizer and out of the drain. In order to increase the amount of water added in the air stream, water vapor is introduced to coflow with the air.

2. Two-Stage Methane Air Flame

As described in our previous work and as shown in Figure I, this two-phase laminar counterflow configuration exhibits a green premixed flame, a blue diffusion flame, and a vaporization plane. All three are flat and parallel. The separation distances between them decrease with increasing equivalence ratio and strain rate. Since the distance between the two flames is as large as 6 mm, it is easier for probes to obtain reliable experimental results with good spatial resolution.

3. Measurements

The species H_2, O_2, N_2, CH_4, CO, CO_2, C_2H_2. C_2H_4 and C_2H_6 are measured by a Varian 3600 gas chromatograph. Centerline temperature pro-files in the present two-stage flame are measured by a Pt-6%Rh vs. Pt-30%Rh thermocouple. Velocity fields and spray structure are measured by the PDPA. The measured small droplet velocity is used to determine the strain rate in air side. By regulating the total flow rates of the two streams, the strain rate in the present experiment is adjusted to be about $50s^{-1}$ based on the PDPA measurement. All details for these measurement techniques were discussed in our previous publications [10, 11].

A No_x analyzer (Model 955, Rosemount Analytical Inc.), is employed for measuring concentrations of NO andNo_x. The analyzer can be operated at a low flow rate of sample so that the disturbance to flame structure can be reduced to a negligible level. The quartz micro-sampling probe for the analyzer is a standard type as described by Saito et al. [12], and it is mounted on a two-dimensional positioner to fix the probe at the desired location. The inner diameter of the probe tip is smaller than 0.I mm. Samples are withdrawn from the flame by the analyzer continuously at a flow rate of approximately 0.4 cc/sec. Because the sample flow rate is low, the response time of the analyzer is about three minutes at a given probe position. The analyzer is calibrated before the experiment and is checked by the calibration gas once every hour during the measurement to ensure that the analyzer performs accurately.

RESULTS

1. The Reaction Pathways

Figure 2 shows the reaction path for $\Phi = 3$ and $a = 50\ s^{-1}$ without water addition at normal atmospheric pressure. While specific information in the figure is associated with this condition, the general scheme applies over a wide range of conditions for which two-stage flames exist. The fractions(in parentheses) are obtained by

integrating consumption rates over the entire field, including both flames. It is seen here that H_2 68.9%, 25.5%, and 5.5% of the methane is consumed by H, OH, and O, respectively to form CH_3. The CH_3, the first product of methane, goes to C_2H_6, CH_3H_5, CH_2O $^1CH_2$, $^3CH_2$, CH_2OH, and CH_3O which eventually are oxidized to CO_2. The CH radical, which is the primary source for prompt No_x, is formed by the reactions of $^3CH_2$ with H and OH while the $^3CH_2$ is produced from CH_3, $C2H_2$ and $^1CH_2$. This is true not only for methane but for higher hydrocarbons. The CH radicals are mainly consumed by H_2O, CO_2 and O_2. In this example, 67%, 20%, and 9% of the CH are oxidized to form CO, CHO, and C H_2O by H_2O, CO_2 and O_2, respectively, and only about I% of the CH is consumed by N_2 to form N and HCN. It is clear that the concentration of the CH radicals can be reduced by increasing the concentrations of H_2O, and CO_2 in the region where the CH radicals are produced.

2. Flame Structure

Figures 3a and 3b for Φ = 1.5 and Figures 4a and 4b for Φ =2.5 show both measured and computed profiles of temperature and concentrations. We see from Figures 3a and 4a that methane and oxygen in the rich mixture react very rapidly to form CO and H_2, and their mole fractions reach maxima as methane disappears. This occurs in the green flame as shown in Figure 1. The further oxidation of CO and H_2 to form CO_2 and H_2O occurs in the diffusion flame which is characterized by the blue emission as shown in Figure 1. The C_2 species, such as C_2H_2, C_2H_4, and C_2H_6 are produced rapidly in the front of premixed flame as shown in Figures 3b and 4b. However these species have very short lives, and they cannot be found experimentally in the diffusion flame. Figures 3b and 4b clearly show that the concentrations of C_2 species strongly depend on the equivalence ratio; the richer the flame is. the higher is the concentration of C_2 species, consistent with observed soot emissions in fuel-rich methane-air flames. The agreement between experiment and prediction is very good for temperature and most of species.

There are some quantitative disagreements for H_2 and C_2H_2 and C_2H_4. The measured concentrations are always lower than the predicted. This is especially true for lower equivalence ratio. Further work is needed on this issue.

Since radicals such as H, OH, O, and CH play dominant roles in hydrocarbon flames, knowledge of their distributions in the flame should help in under-standing flame structure andNo_x formation. Figures 3b and 4b also show predicted profiles of their concentrations. These figures indicate that the concentrations of C_2 species peak in the premixed flame, the cooler flame, while the radicals H, OH, and O have the highest concentrations in the diffusion flame, the hotter flame. The CH concentration peaks between the premixed and diffusion flames. It is noted that there are two peaks for the concentration profiles of CH, H,and OH for the lower equivalence ratio as shown in Figure 3b, while those radicals have only one peak for the higher equivalence ratio as shown in Figure 4b. This is a very important character for the two-stage combustion.

3. Influence of Water and CO_2 on the Concentration of CH

As shown in Figure 2, the concentrations of CH radicals are directly controlled by the reactions

$$1 \quad CH + H_2O \rightleftharpoons CH_2O + H$$

$$2 \quad CH + O_2 \rightleftharpoons CHO + O$$

$$3 \quad CH + CO_2 \rightleftharpoons CHO + CO$$

$$4 \quad {}^3CH_2 + H \rightleftharpoons CH + H_2$$

$$5 \quad {}^3CH_2 + OH \rightleftharpoons CH + H_2O$$

where the first three consume CH and the last two produce it. It is clear that when the water and CO_2 are added to the region where CH radicals are produced the CH concentration can be significantly reduced. Computation results shown in Table 1 indicate how additions of water, CO_2, N_2, and Argon influence the maximum concentrations of CH radicals in two-stage combustion. For comparison, results of zero addition are also listed. It is found that both water and CO_2 are much more effective in reducing CH than nitrogen and Argon and that, for a given mass percentage of addition, water is the most effective agent for large Φ. For instance, addition of 10% water in the flame with

Φ = 3 can change the maximum of CH from 8.3×10^{-7} to 3.9×10^{-7}, more than 50%. The concentration of the CH is insensitive to additions of nitrogen and Argon. It is also found that additions of water and CO_2 become less effective in reducing CH when fuel concentration decreases in the methane-air stream. For example, additions of water and CO_2 have only minor influence on the maximum values of CH in the flames with Φ = 1.5. This means that the added agents in the air stream are not able to get into the region where the CH radicals are produced when the two flames are separated far apart.

4. Influence of Water Addition on No_x Formation

The experimental measurements as in Figures 5-8 have shown that the maximum concentrations of NO are always found near the blue diffusion flame and that they can be significantly reduced by adding water in the pure air stream. For example, the measured maximum NO concentrations were 69, 89, 100, 90 ppm for Φ = 1.5, 2.0, 2.5 and 3.0, respectively, at $a = 50\ s^{-1}$. On the other hand, by adding 5% of water into the pure air stream, these maximum NO concentrations were reduced to 60, 70, 50, and 40 ppm, respectively, without changing other conditions. In general, the agreements between experimental measurement and numerical prediction are reasonably good.

5. Influence of Water Addition on the Emission Index

The NO emission index is defined as

$$E_{NO} = \frac{1000 \int_{-L_s}^{L_s} M_{NO}\, \dot{\omega}_{NO}\, dz}{-\int_{-L_s}^{L_s} M_{CH_4}\, \dot{\omega}_{CH_4}\, dz} \quad \left(\frac{g}{kg - CH_4}\right),$$

where $-\dot{\omega}CH_4$ is the total consumption rate of methane and $\dot{\omega}_{NO}$ is the total production rate of NO, and M_{NO} and M_{CH_4} are the molecular weights of NO and CH_4, respectively. Figure 9 plots the predicted E_{NO} as a function of Φ at a strain rate of $50\ s^{-1}$ with adding 0, 5%, and 10% water, CO_2, N_2 and Argon in the air stream. It can be seen that water is the most effective agent in reducing NO emission. The effect of agent types on emission of NO varies as

$H_2O > CO_2 >> N_2 > Ar$.

The latter two agents reduce No_x emission through reducing flame temperature while the former two reduce No_x emission through reducing not only flame temperature but also prompt No_x. Another feature shown in Figure 9 is that the additions of water and CO_2 are always more effective in reducing No_x when Φ is large. All these are consistent with the data shown in Table 1.

CONCLUSIONS

Well-defined two-stage flames in counterflowing streams have been employed in testing a chemical-kinetic data base for H-C-N-O combustion systems recently compiled and validated. Both experimental and numerical prediction have indicated that the water vapor added in the air stream helps to increase the water concentration in the flame zone and thus reduce the concentration of CH radicals. The present work reveals that prompt NO in the present two-stage counterflow combustion plays a dominant role in No_x formation and that the No_x emission index strongly depends on the flame structure and on the mass fraction of water and CO_2 added in the air stream. The No_x emission index can be substantially reduced by adding water and CO_2 in the region where CH radicals are produced.

ACKNOWLEDGMENT

This research was supported by the Department of Energy, Office of Basic Energy Sciences, Division of Engineering and Geosciences under contract DE-F003-87ERI3685 and BKM, Inc. and South Coast Air Quality Management District under contract AB2766/97006.

REFERENCES

1. Langston, L., "Market drivers for electric power gas turbines: Reasons for the revolution." *Global Gas Turbine News,* Vol. 36, No.3, pp.7-10, 1996.

2. Bogdanoff, M.A.,"Diesel Engines and Emission Reduction Programs," *Proceedings of the 1995 Diesel Engine Emissions Reduction Workshop,* pp.I31-I39, University of California-San Diego, La Jolla, July 24-27, 1995,

Sponsored by Office of Transportation Technologies of U.S. Department of Energy.

3. Ilincic, N. and Li, S.C., "Influence of Water and CO_2 Addition on NO_x formation in Partially Premixed Flames," Western States Section/The Combustion Institute, 1995 Fall Meeting.

4. Smooke, M.D., Crump, J., Seshadri, K. and Giovangigli, V., "Comparison between Experimental measurements and Numerical Calculations of the Structure of Counterflow, Diluted, Methane-Air, Premixed Flames," Twenty-Third Symposium (International) on Combustion, The Combustion Institute, Pittsburgh, 1990, pp.463-470.

5. Pitsch, H., *Entwicklung eines Programm paketes zur Berechnung eindimensionaler Flammen am Beispiel einer Gegenstormdiffusionsflamme.* Masters thesis, RWTH, Aachen, Germany, 1993.

6. Balakrishnan, G. and Williams F.A. "Turbulent Combustion Regimes for Hypersonic Propulsion Employing Hydrogen-Air Diffusion Flames," Journal of Propulsion and Power 10, 434 (1994).

7. Rightley, M.L. and Williams, F.A., "Analytical Approximations for Structures of Wet CO Flames with One-Step Reduced Chemistry," *Combustion and Flame* 101, 287 (1996).

8. Rightley, M.L. and Williams, F.A., "Structures of CO Diffusion Flames Near Extinction " to appear in *Combustion Science and Technology,* (1997).

9. Li, S.C., Williams, F.A., and Ilincic, N., "Experimental and Numerical Studies ofNo_x Formation in Two-Stage Methane Flames," work in Progress, 1997.

10. Li, S.C., Ilincic, N., and Williams, F.A., " Reduction of NO_x Formation by Water Sprays in Strained Two-Stage Flames," presented at ASME TURBO-EXPO'96, Birmingham, England, UK, June 10-13, 1996, ASME Paper 96-GT-545 and to appear in *ASME Journal of Engineering for Gas Turbines and Power.* October, 1997.

11. Li, S.C. and Williams, F.A., "Experimental and Numerical Studies of Two-Stage Methanol Flames," *Twenty-Sixth Symposium (International) on Combustion, Naples* Italy, July 28 - August 2, 1996, pp. I0I7-I024.

12. Saito, K., Williams, F.A., and Gordon, A.S., "Structure of Laminar Coflow Methane-Air Diffusion Flames," *J. Heat Transfer,* 108, 640 (1986).

Table1: Maximum mole fraction of CH radical uder different additions of water, CO_2 and nitrogen.

Φ	Zero	H_2O		CO_2		N_2		Ar	
	Addition	5%	10%	5%	10%	5%	10%	5%	10%
1.5	1.5×10^{-7}	1.4×10^{-7}	1.4×10^{-7}	1.5×10^{-7}	1.5×10^{-7}	1.5×10^{-7}	1.5×10^{-7}		
2.0	3.7×10^{-7}	3.0×10^{-7}	2.4×10^{-7}	3.6×10^{-7}	3.4×10^{-7}	3.6×10^{-7}	3.6×10^{-7}		
2.5	6.5×10^{-7}	4.9×10^{-7}	3.6×10^{-7}	5.9×10^{-7}	5.4×10^{-7}	6.3×10^{-7}	6.0×10^{-7}		
3.0	8.3×10^{-7}	5.9×10^{-7}	3.9×10^{-7}	7.4×10^{-7}	6.4×10^{-7}	8.0×10^{-7}	7.5×10^{-7}		
∞	2.0×10^{-6}	1.1×10^{-6}	4.5×10^{-7}	1.5×10^{-6}	9.9×10^{-7}	1.8×10^{-6}	1.4×10^{-6}	2.0×10^{-6}	1.8×10^{-6}

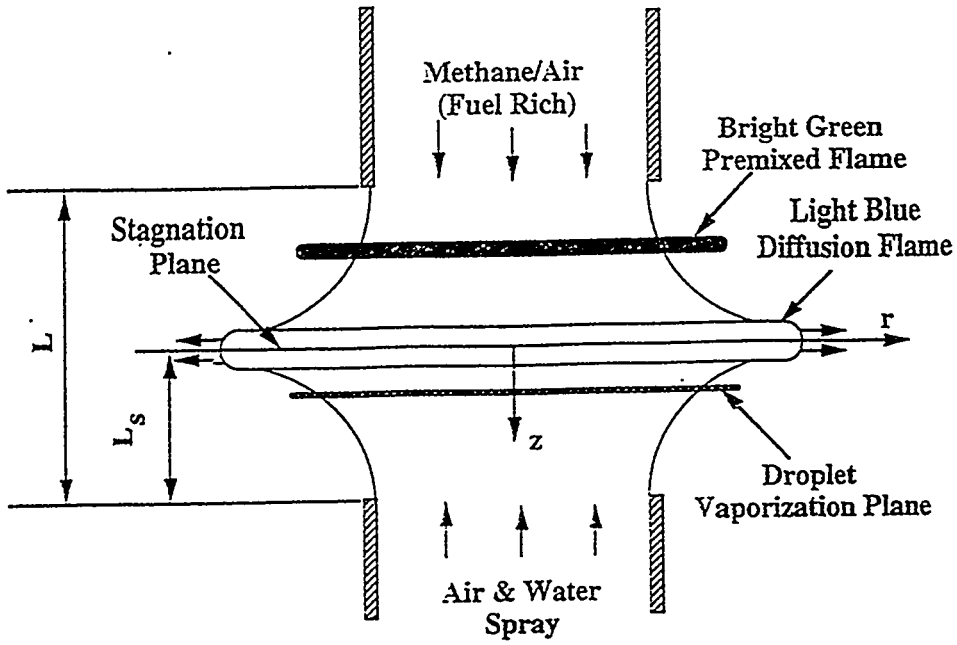

Fig.1: Sketch of a two-stage methane-air flame in water spray counterflow streams.

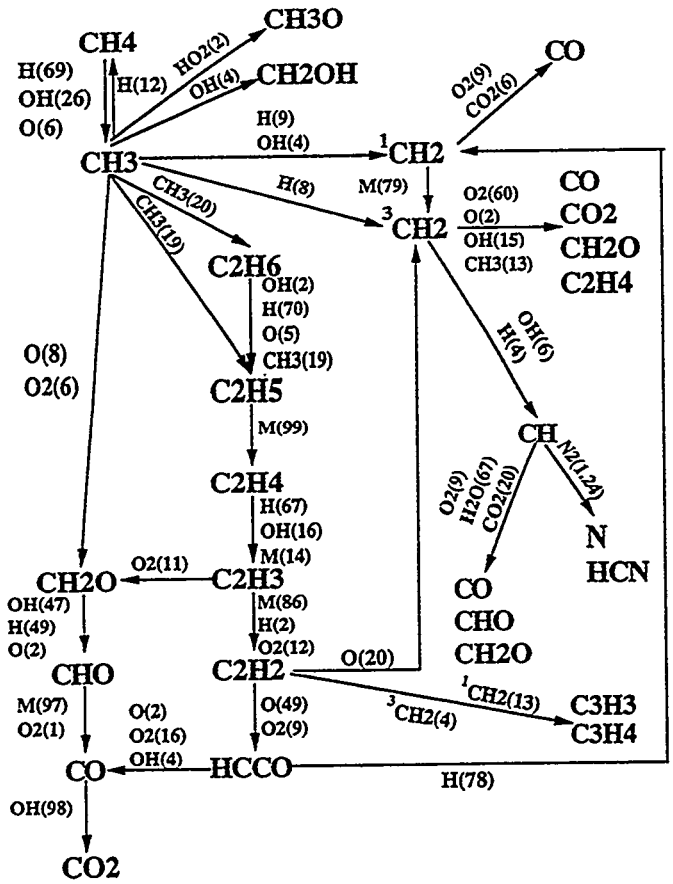

Fig.2: Reaction path of methane in two-stage methane-air flame with Φ= 3.

Fig.3a: Comparison between measurement and prediction for concentration profiles for Φ=1.5 and a = 50 s^{-1}.

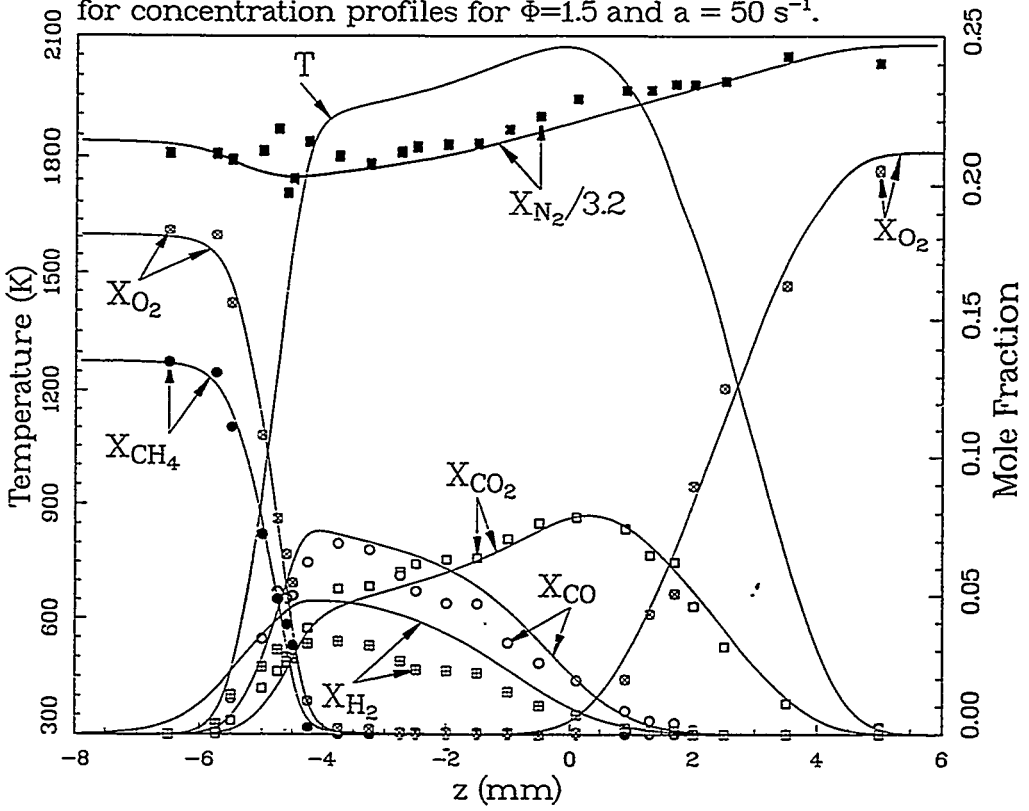

Fig.3b: Comparison between measurement and prediction for profiles of temperature and concentrations of radicals and C_2 species for Φ=1.5 and a = 50 s^{-1}.

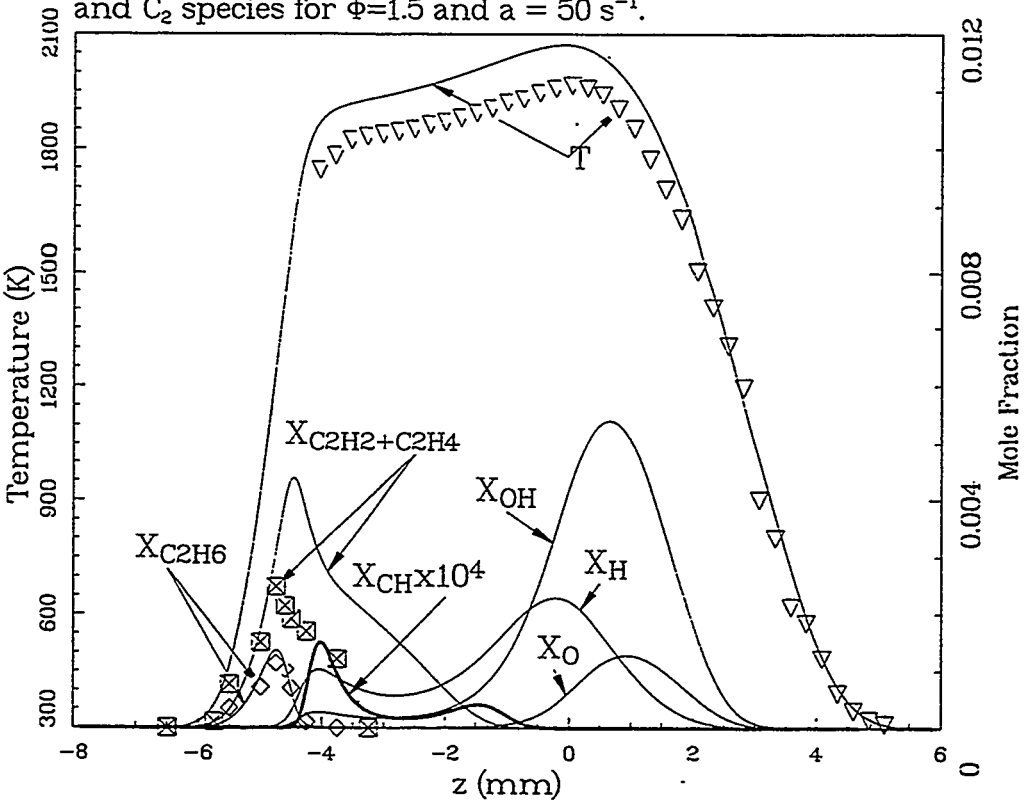

Fig.4a: Comparison between measurement and prediction for concentration profiles for Φ=2.50 and a = 50 s^{-1}.

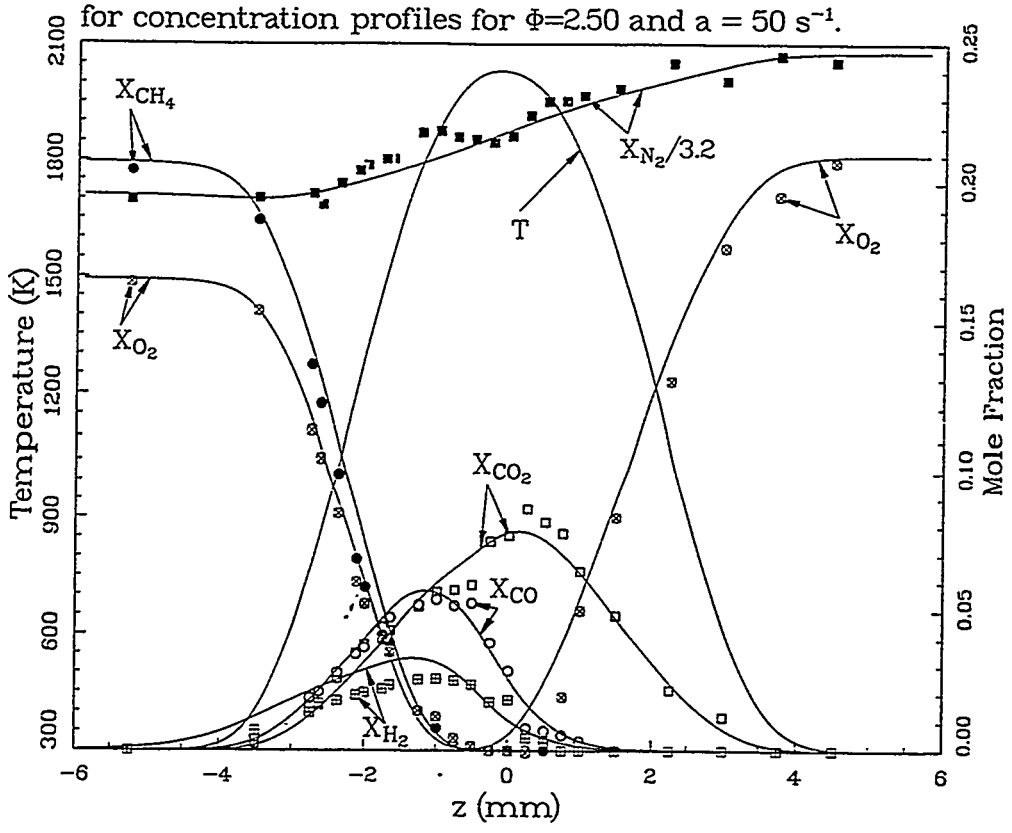

Fig.4b: Comparison between measurement and prediction for profiles of temperature and concentrations of radicals and C_2 species for Φ=2.5 and a = 50 s^{-1}.

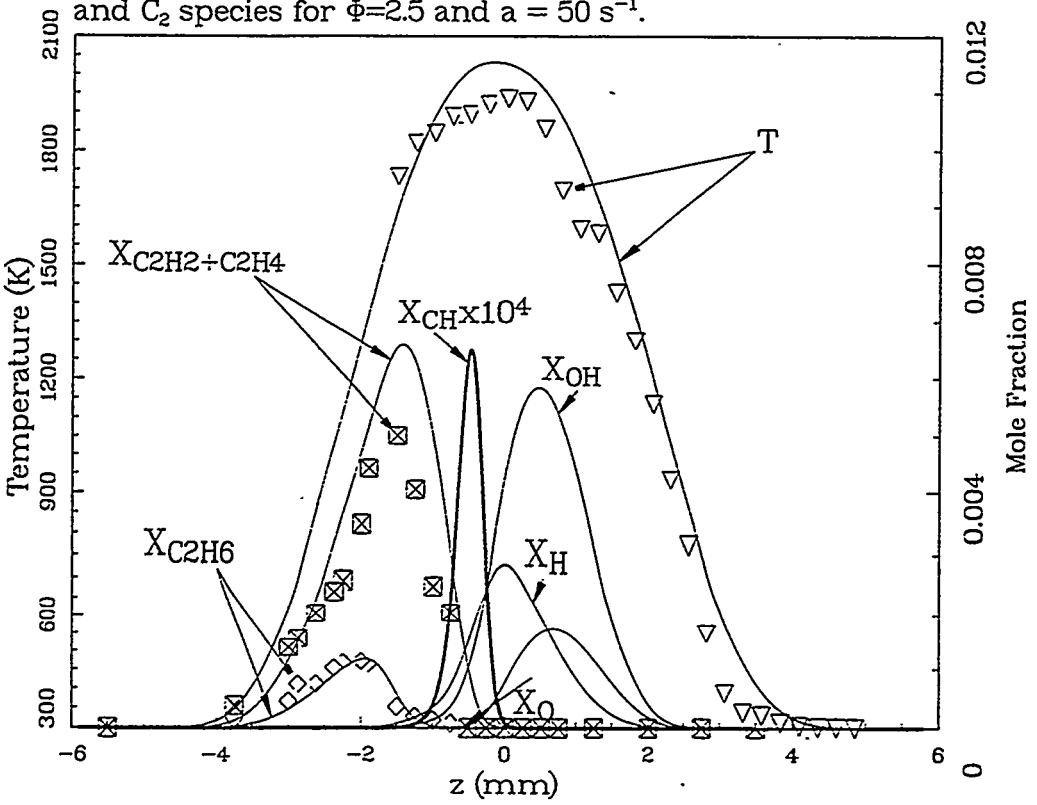

Fig.5: Comparison between measurement and prediction for profiles of NO concentration and temperature on the axis with Φ= 1.50 and strain rates of 50 s^{-1}.

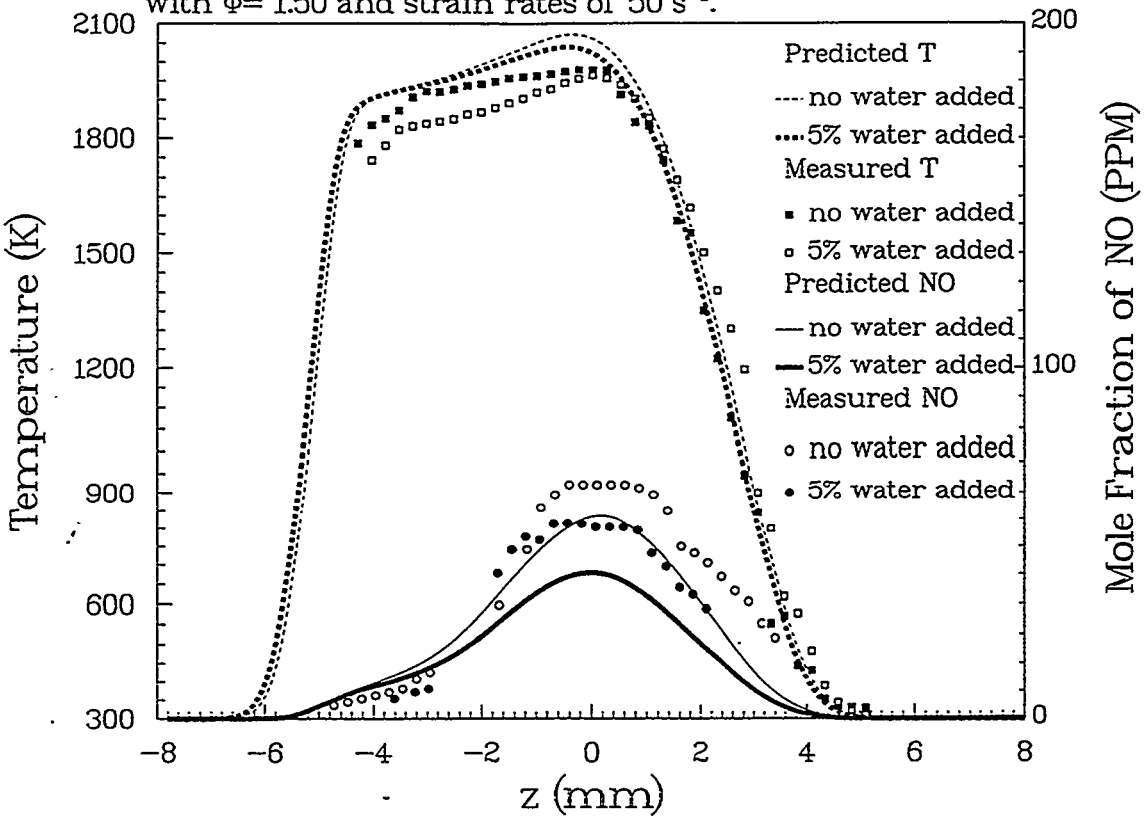

Fig.6: Comparison between measurement and prediction for profiles of NO concentration and temperature on the axis with Φ= 2.00 and strain rates of 50 s^{-1}.

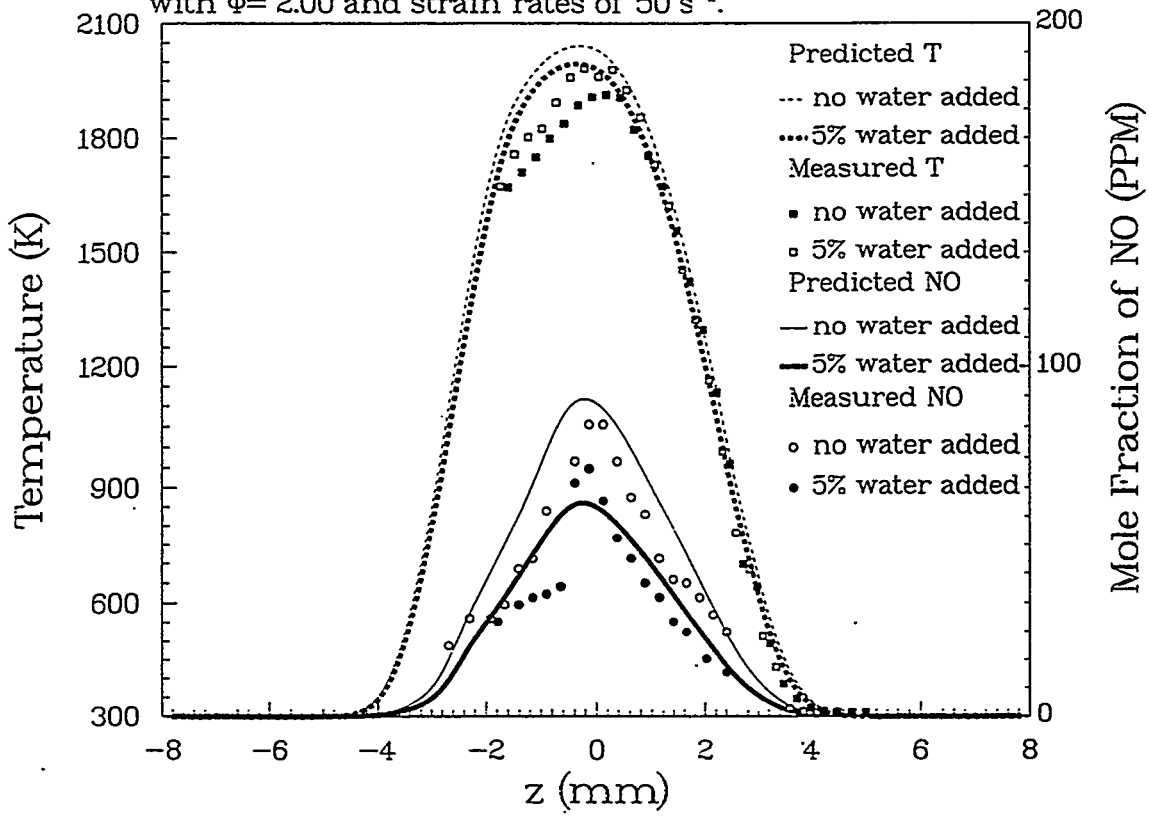

Fig.7: Comparison between measurement and prediction for profiles of NO concentration and temperature on the axis with Φ= 2.50 and strain rates of 50 s^{-1}.

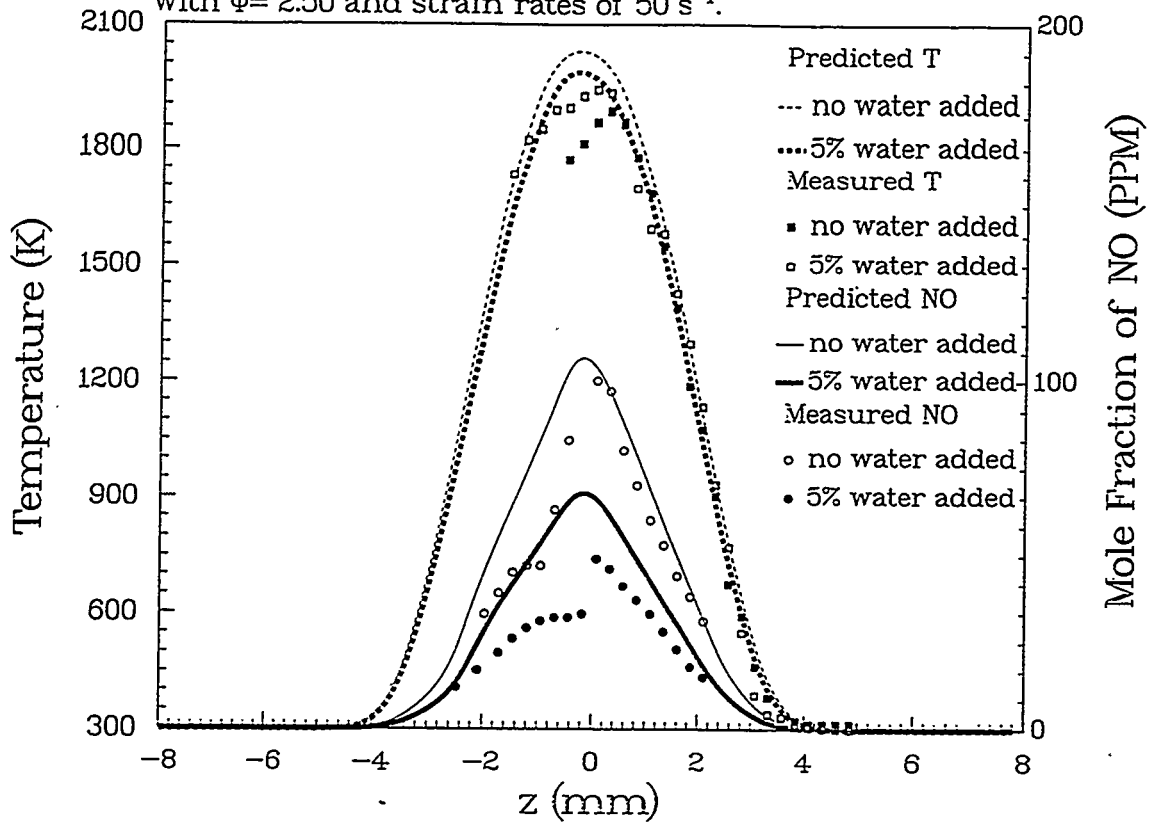

Fig.8: Comparison between measurement and prediction for profiles of NO concentration and temperature on the axis with Φ= 3.00 and strain rates of 50 s^{-1}.

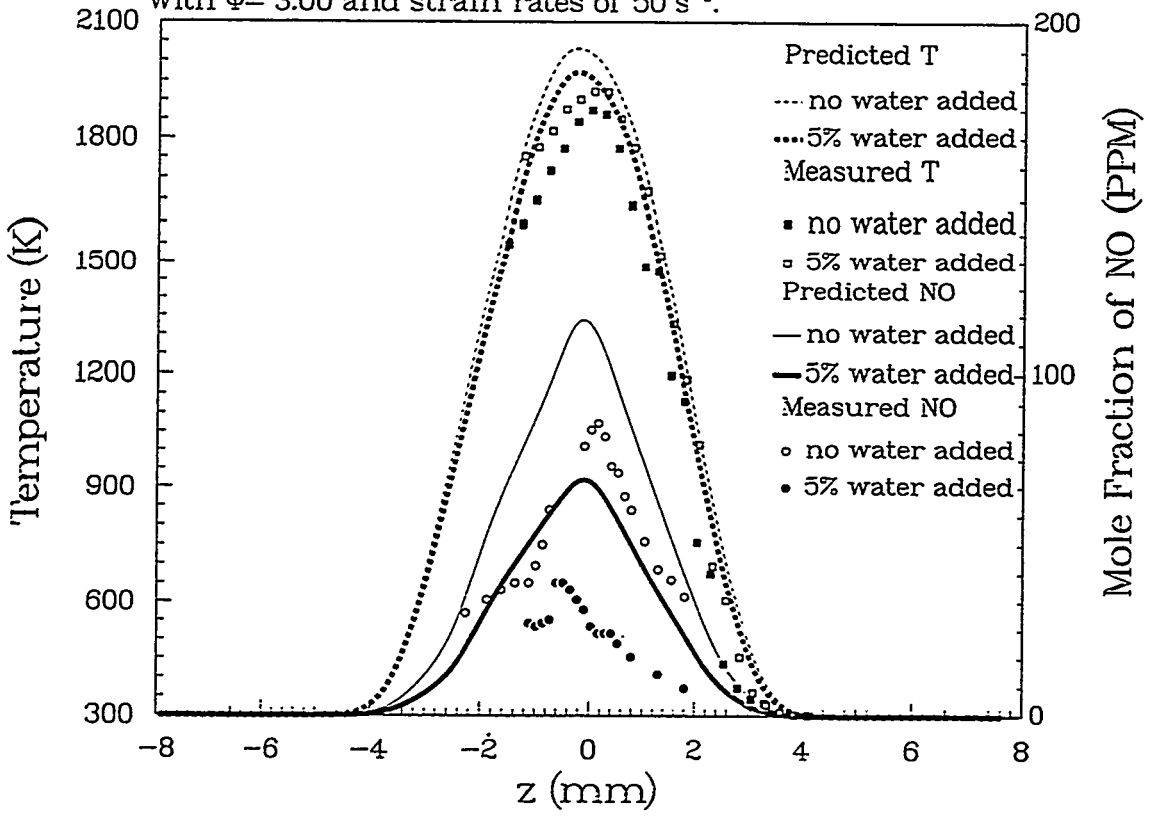

Fig.9: Predicted NO emission index as a function of equivalence ratio with water and CO_2 added to the air stream.